Diphosphorylation of the Myosin Regulatory Light Chain Enhances the Tension Acting on Stress Fibers in Fibroblasts

Takeomi Mizutani,[1,*] Hisashi Haga,[1] Yoshikazu Koyama,[2] Masayuki Takahashi,[3] and Kazushige Kawabata[1]

[1] *Division of Biological Sciences, Graduate School of Science, Hokkaido University, North 10 West 8, Kita-ku, Sapporo 060-0810, Japan*

[2] *Department of Biochemistry, Graduate School of Medicine, Hokkaido University, North 15 West 7, Kita-ku, Sapporo 060-8638, Japan*

[3] *Division of Chemistry, Graduate School of Science, Hokkaido University, North 10 West 8, Kita-ku, Sapporo 060-0810, Japan*

Journal type: **Rapid Communications**

*Correspondence to: Takeomi Mizutani

Division of Biological Sciences, Graduate School of Science,

Hokkaido University, Sapporo 060-0810, JAPAN

Telephone: +81-11-706-4483

FAX: +81-11-706-4992

E-mail: mizutani@sci.hokudai.ac.jp

Running Title: Increment of force by diphosphorylated MRLC

Key words: **myosin regulatory light chain; scanning probe microscopy; diphosphorylation; contractile force; Rho-associated kinase;**

Total number of text figures: 5 figures

Total number of tables: 0 tables

1st Grant informations: Contract grant sponsor: the Japan Science Society; Contract grant number: 17-203

2nd Grant informations: Contract grant sponsor: the Ministry of Education, Culture, Sports, Science and Technology of Japan; Contract grant number: 14GS0301

ABSTRACT

Regulation of the contractile force is crucial for cell migration, cell proliferation, and maintenance of cell morphology. Phosphorylation of the myosin II regulatory light chain (MRLC) is involved in these processes. To show whether the diphosphorylation of MRLC increases the tension acting on stress fibers, changes in the stiffness of fibroblasts expressing wild-type MRLC and a mutant type, which cannot be diphosphorylated, on treatment with lysophosphatidic acid (LPA) were examined by a mechanical-scanning probe microscope (M-SPM). The LPA treatment increased cellular stiffness in the wild-type MRLC expressing cells, while it had no effect on the mutated cells. Immunostaining showed that LPA stimulation induced the diphosphorylation of MRLC. These results suggest that the diphosphorylation of MRLC enhances the tension acting on stress fibers.

INTRODUCTION

In eukaryotic cells, contractile force is important for the performance of a large variety of physiological functions such as cell movement, cytokinesis, and maintenance of cell morphology. One of the main generators of the contractile force is the interaction between actin filaments and myosin II, in which the phosphorylation of the myosin II regulatory light chain (MRLC) is essential (Ikebe et al., 1986; Somlyo and Somlyo, 2003). Two phosphorylatable sites—threonine 18 and serine 19—are responsible for the activation of the myosin motor activity of MRLC. Serine 19 is more easily phosphorylated than threonine 18, allowing MRLC to be in either the de-, mono-, or diphosphorylated state (Ikebe et al., 1986). Earlier reports showed that myosin II in diphosphorylated MRLC (PP-MRLC) has a higher actin-activated Mg^{2+}-ATPase activity than that in monophosphorylated MRLC (P-MRLC) (Ikebe et al., 1988; Umemoto et al., 1989). In addition, several biochemical differences between the *in vitro* phosphorylated MRLCs were reported (Colburn et al., 1988; Trybus, 1989); however, a clear distinction between the phosphorylated MRLCs in the generation of contractile force has not been elucidated.

To measure the contractile force in a single cell, we used a mechanical-scanning probe microscope (M-SPM), which can visualize the spatial distribution of stiffness reflected by the tension in the stress fibers in a cell (Nagayama et al., 2004). By using the M-SPM, we were

successful in observing a dramatic change in cellular stiffness during cell migration (Nagayama et al., 2001) and in discovering tensional homeostasis against external deformation (Mizutani et al., 2004a). Our previous work showed that cellular stiffness increased on stimulation with lysophosphatidic acid (LPA) (Nagayama et al., 2004) that is a RhoA activator. Taking these findings into consideration, we concluded that the phosphorylation of MRLC increases cellular stiffness. However, the manner in which the mono- and diphosphorylation of MRLC contribute to the contractile force is unclear.

The purpose of this study was to examine whether PP-MRLC induces a higher *in vivo* contractile force than P-MRLC. We measured the stiffness of cells expressing green fluorescent protein (GFP)-tagged wild-type MRLC ($MRLC^{WT}$-GFP) and a mutant type, which cannot be diphosphorylated ($MRLC^{T18A}$-GFP), before and after LPA stimulation.

MATERIALS AND METHODS

Cell culture and sample preparations

Fibroblasts (NIH-3T3) were purchased from the RIKEN Cell Bank (Tsukuba, Japan) and cultured in low glucose Dulbecco's modified Eagle's medium (DMEM) supplemented with 10% heat-inactivated bovine serum and 1% antibiotics (Invitrogen, Carlsbad, California) in 5% CO_2 at 37 $^{\circ}$C. The cells were trypsinized and plated onto a glass dish coated with fibronectin (Boehringer Mannheim, Mannheim, Germany). Prior to M-SPM or immunofluorescence measurements, the culture medium in the dishes was replaced with DMEM buffered with serum-free HEPES (Sigma-Aldrich, St. Louis, Missouri) for 12 h. The cells were treated with 10 μM LPA (Sigma-Aldrich), 40 μM of the myosin light chain kinase (MLCK) inhibitor ML-7 (CALBIOCHEM, Fullerton, California), or 10 μM LPA + 40 μM ML-7 in HEPES buffer at suitable timings during the measurements. Although such an excess dose of ML-7 may cause the inhibition of both protein kinase A and protein kinase C (Krarup et al., 1998), the aim of the excess treatment performed here was to completely abolish the activity of the MLCK.

Construction of recombinant plasmids and transfection procedure

The cDNA of wild-type nonmuscle MRLC (GenBank accession no. *BC004994*) was obtained from a human brain cDNA library (BD Biosciences Clontech, Mountain View,

California) using PCR, as described elsewhere (Yuasa et al., 2002). The cDNA fragment of the wild-type nonmuscle MRLC was subcloned into a pEGFP-N3 (BD Biosciences Clontech) vector. To generate two mutant MRLCs (termed as $MRLC^{T18A}$-GFP and $MRLC^{T18D, S19D}$-GFP), a part of the MRLC sequence was substituted using PCR. $MRLC^{T18A}$-GFP in which the diphosphorylation of MRLC was prevented was constructed by the substitution of threonine 18 to alanine 18. $MRLC^{T18D, S19D}$-GFP in which MRLC was constitutively diphosphorylated was constructed by the following substitutions: threonine 18 to aspartic acid 18 and serine 19 to aspartic acid 19. To construct GFP-not-tagged MRLC, the cDNA fragment of wild-type MRLC or $MRLC^{T18A}$ was substituted for the GFP fragment in the pEGFP-N3 vector. A plasmid coding for both dominant-negative RhoA and the DsRed expression marker (pIRM21-Flag-Rho^{N19}) was kindly provided by Dr. M. Matsuda (Osaka University) (Aoki et al., 2004). All the plasmids were purified by cesium chloride density gradient centrifugation in order to obtain high protein expression. Cells were transfected using the Effectene transfection reagent (QIAGEN, Valencia, California) according to the manufacturer's instructions. Briefly, cells cultured at a concentration of 30 cells/mm^2 in a plastic flask were treated with 1 μg/mL of cDNA complexed with the Effectene reagent in the culture medium. The maximum efficiency of expression was achieved more than 1 day after the transfection.

Stiffness measurements with M-SPM

The M-SPM used in this study, known as a wide-range SPM, is a modification of the commercial SPM (SPA400; Seiko Instruments Inc., Chiba, Japan) and is equipped with a tandem piezo scanner with a maximal scan range of 500 μm (*xy* axis) and 26 μm (*z* axis) (Mizutani et al., 2004b). A silicon-nitride cantilever with a spring constant of 0.01 N/m (MLCT-AUNM; Veeco, Woodbury, New York) was used. The spatial distribution of cellular stiffness was imaged in the force mapping mode, as described previously (Haga et al., 2000; Radmacher et al., 1996). In brief, this mode can simultaneously provide both the height and stiffness images of a sample by generating a force curve at each pixel point in a scan area consisting of 64 pixels × 64 lines. The local stiffness (Young's modulus) of the sample was evaluated quantitatively from a force curve that was fitted to the Hertz model by using a nonlinear least-squares method. During the measurements, a petri dish filled with HEPES buffer was maintained at physiological temperature. The dish was placed on a metal plate maintained at 37 $^{\circ}$C by a temperature controller that consisted of a heater and a thermocouple.

To obtain the representative stiffness of a cell in each experiment, one set of height and stiffness images was used. The highest point in a height image was defined as the center of the cell. The stiffness values within a circular area of 100 μm^2 from this point were averaged. Statistical changes in the averaged stiffness were examined using Student's *t*-test. These data

were presented as mean ± SEM.

Immunofluorescence analysis

Cells were rinsed with phosphate-buffered saline (PBS, Invitrogen), followed by fixation with 4% formaldehyde/PBS for 10 min. They were then washed twice with PBS and permeabilized with 0.5% Triton X-100/PBS for 10 min. After blocking the nonspecific binding sites with 0.5% bovine serum albumin (BSA, Invitrogen) in PBS, the cells were stained with specific primary antibodies/PBS by incubation for 1 h on a mild shaker. Subsequently, the cells were rinsed three times with PBS containing 0.5% BSA and stained with secondary antibodies/PBS by incubation for 1 h on the same shaker. To avoid loss of fluorescence intensity, the cells were covered with 1,4-diazobicyclo[2.2.2]octane (DABCO; Wako Pure Chemicals, Osaka, Japan) diluted in glycerol. Fluorescence images were obtained with a confocal laser scanning microscope (C1 confocal imaging system; NIKON Instech Co., Ltd., Tokyo, Japan). Sectional images were collected and processed using the EZ-C1 software (NIKON Instech).

To quantify the degree of MRLC diphosphorylation, the fluorescent intensity of PP-MRLC was measured using a commercial software (Image-Pro Plus; Media Cybernetics, Silver Spring, Maryland). In the fluorescent image, the contour of a cell was traced manually. The intensities of PP-MRLC in a cell were averaged, in which unlikely signals from the nucleus

were eliminated. Statistical changes in the averaged intensity were examined using Student's *t*-test. These data were presented as mean ± SEM.

Electrophoresis and western blotting

Cells cultured in flasks were quickly washed with cold PBS and were then frozen at –20 °C. Trichloroacetic acid (10% w/v) (Wako Pure Chemcals) was added to the flask. The cells were scraped 10 minutes after the application. To demineralize the cell pellet, acetone (Wako Pure Chemicals) was added to it and the mixture was centrifuged. We applied two types of sample buffers to the pellet depending on the electrophoresis method followed. For sodium dodecyl sulfate polyacrylamide gel electrophoresis (SDS-PAGE), the sample buffer consisted of 125 mM Tris-HCl, pH 6.8; 2.3% (w/v) SDS; 10% (w/v) glycerol; 5% (w/v) dithiothreitol; and 10 μg/mL bromophenol blue. For urea-PAGE, the sample buffer consisted of 20 mM Tris-glycine, pH 8.6; 8 M urea; 5% (w/v) dithiothreitol; and 10 μg/mL bromophenol blue (Daniel and Sellers, 1992). The above agents were purchased from Wako Pure Chemicals. These samples were sonicated and then stored at –20 °C.

SDS-PAGE was performed following standard procedures. Urea-PAGE was performed as described previously (Daniel and Sellers, 1992). In brief, the samples were applied to a 16 cm × 16 cm urea gel and were electrophoresed for 5 h at 10 W, 500 V. Proteins were transferred to a

PVDF membrane by semidry blotting carried out for 1 h at 1 mA/cm^2 with a transfer buffer comprising 20 mM Tris-glycine, pH 8.6 and 6 M urea. After the SDS- and urea-PAGE, the membranes were washed with 0.05% polyoxyethylene (20) sorbitan monolaurate (Wako Pure Chemicals) in PBS and blocked with 1% BSA in PBS for 30 min. Immunoreactive proteins were detected using an enhanced chemiluminescent detection system according to the manufacturer's protocol (Amersham, Little Chalfont, UK). Images of protein blots were processed using Image-Pro Plus (Media Cybernetics).

To show the change in P-MRLC in urea-PAGE, the increase was calculated from

$$I = \frac{A_{P-MRLC} / A_{total-MRLC}}{B_{P-MRLC} / B_{total-MRLC}}, \quad (1)$$

where the notations are as follows: I, the increase in P-MRLC; $A_{p\text{-}MRLC}$, intensity of P-MRLC with LPA treatment; $A_{total\text{-}MRLC}$, intensity of total MRLC with LPA treatment; $B_{p\text{-}MRLC}$, intensity of P-MRLC without LPA treatment; and $B_{total\text{-}MRLC}$, intensities of total MRLC without LPA treatment.

Antibodies

Phosphorylated MRLCs were detected by the following antibodies: anti-P-MRLC (#3671; Cell Signaling Technology, Beverly, Massachusetts) that reacted with P-MRLC^{T18A},

P-MRLC and PP-MRLC; anti-PP-MRLC (#3674; Cell Signaling Technology) that reacted with only PP-MRLC. An antibody that reacted with MRLC and MRLC-GFP was purchased from Cell Signaling Technology. Anti-α-tubulin specific for tubulin was purchased from Sigma-Aldrich. Fluorescently conjugated secondary antibodies as well as fluorescently tagged phalloidin were purchased from Invitrogen. Horseradish peroxidase (HRP)-conjugated secondary antibodies used for western blotting were purchased from Bio-Rad Laboratories (Hercules, California).

RESULTS

To confirm whether the overexpression of MRLC^{T18A}-GFP was able to prevent the diphosphorylation of MRLC, cells transfected with MRLC^{T18A}-GFP were incubated for 1 h in HEPES buffer containing LPA, following which immunofluorescence staining for PP-MRLC was performed (Fig. 1A). Although the cells expressing MRLC^{T18A}-GFP showed fibrous MRLC structures, these structures were not stained with the anti-PP-MRLC antibody in both with and without LPA. The expression ratio of exogenous to endogeneous MRLC was confirmed by western blotting (Fig. 1B). The expression level of exogenous MRLC was greater than that of endogenous MRLC. These results indicate that overexpressed MRLC^{T18A}-GFP cannot be diphosphorylated.

To elucidate whether the intracellular tensional force in the cells expressing MRLC^{T18A}-GFP changes after LPA stimulation, we measured cellular stiffness before and 1 h after the LPA treatment. Figure 2A shows the change in the stiffness of the cells expressing MRLC^{T18A}-GFP or MRLC^{WT}-GFP as measured by the M-SPM. Stiffer fibrous structures corresponding to the stress fibers were observed in both the images. In the cells expressing MRLC^{T18A}, LPA stimulation did not alter cellular stiffness, whereas the cells expressing MRLC^{WT} had stiffened after LPA stimulation, as previously reported (Nagayama et al., 2004). In particular, the regions indicated by the arrows in Fig. 2A had stiffened after LPA stimulation.

The cellular stiffness in each image was averaged over the central area (see materials and methods) of the cellular surface to quantify the degree of change in stiffness due to the LPA treatment. The averaged stiffness before and after the LPA treatment was plotted (Fig. 2B). There was a significant difference in cellular stiffness between $MRLC^{T18A}$- and $MRLC^{WT}$-expressing cells after LPA treatment, although there was little difference between these cells in this regard before LPA stimulation. Statistical analysis showed that the stiffness of cells expressing $MRLC^{T18A}$ did not change after LPA stimulation. To strengthen the effect of the diphosphorylation of MRLC on stiffness, we measured the stiffness of $MRLC^{T18D, S19D}$-GFP-expressing cells in a serum-free condition. The stiffness of $MRLC^{T18D, S19D}$-expressing cells was found to be greater than that of $MRLC^{WT}$-expressing cells (data not shown). Therefore, the diphosphorylation of MRLC should enhance the intracellular tension due to stress fiber contraction.

To confirm whether LPA stimulation induces the diphosphorylation of endogenous MRLC, normal cells were treated with 10 μM LPA and stained with anti-PP-MRLC and phalloidin (Fig. 3A). All the experiments were performed under starved conditions by using a serum-free medium. Cells stimulated by LPA showed filamentous structures of PP-MRLC, whereas the control cells showed a low amount of PP-MRLC. The structure of the actin filament was observed in LPA-treated or un-treated cells. The intensity of PP-MRLC was quantified (Fig.

3B). Since the antibody for PP-MRLC recognized nuclei (Ueda et al., 2002), immunofluorescence in the nuclear area was excluded from the calculation; however, it was used as a reference level for the immunofluorescence intensity. A significant difference exists between the LPA-stimulated cells and control cells in terms of PP-MRLC. These results indicate that the diphosphorylation of MRLC in stress fibers is involved in the increase in the stiffness change.

There is a possibility that the difference in increase in P-MRLC may contribute to the stiffness change in $MRLC^{T18A}$- and $MRLC^{WT}$-expressing cells. To confirm the change in the amount of P-MRLC by the LPA treatment, we performed a combination of urea-PAGE and SDS-PAGE along with western blotting (Fig. 4A). We used the same amount of samples in urea- and SDS-PAGE in order to compare the relative change in the amount of phosphorylated MRLCs. The amount of PP-MRLC in $MRLC^{WT}$-expressing cells increased with LPA, whereas it did not increase in $MRLC^{T18A}$-expressing cells. The relative change in the amount of P-MRLC was analyzed and is shown in Fig. 4B. There was no significant difference between the $MRLC^{T18A}$- and $MRLC^{WT}$-expressing cells. These results suggest that the diphosphorylation but not the monophosphorylation of MRLC increases the intracellular tension by LPA treatment.

Further, to examine the manner in which LPA stimulation induces the diphosphorylation of MRLC, the involvement of the small GTPase RhoA that regulates the

phosphorylation of MRLC, was tested by using dominant-negative RhoA (Rho^{N19}). The cells expressing Rho^{N19} were examined in the LPA stimulation experiment. The immunofluorescence micrograph of PP-MRLC in a cell expressing Rho^{N19} that was stained after LPA stimulation is shown in Fig. 5A. The diphosphorylation of MRLC by LPA stimulation was inhibited in cells expressing Rho^{N19} (Fig. 5A, B). RhoA is known to be an activator of the Rho-associated kinase (ROCK). ROCK is able to effect myosin II motor activity by both inhibiting MRLC phosphatase (MLCP) *in vivo* (Kimura et al., 1996) and phosphorylating MRLC directly *in vitro* (Amano et al., 1996). In such a case, there are two possibilities for the signal pathways in which MRLC was diphosphorylated by LPA stimulation. One is that MLCK diphosphorylates MRLC because of the inhibition of MLCP activity by ROCK activation and the other is that ROCK diphosphorylates MRLC directly (Matsumura et al., 2001). In order to determine which mechanism is involved, the cells were treated with both ML-7, a known inhibitor of MLCK, and LPA. The cells showed sufficient amounts of PP-MRLC in the stress fibers (Fig. 5C, D). To confirm the effect of ML-7, cells treated only with ML-7 showed a few actin fibers and no phosphorylated MRLC (Fig. 5E, F). Finally, we measured the stiffness of Rho^{N19}-expressing or ML-7 pretreated cells in LPA stimulation. The Rho^{N19} expressing cells did not increase their stiffness, however, ML-7 pretreated cells increased stiffness with LPA (data not shown). These results indicate that ROCK directly induces the diphosphorylation of MRLC via the LPA-RhoA

signaling cascade and enhances the tension of stress fiber.

DISCUSSION

We demonstrated that the diphosphorylation of MRLC enhances the intracellular tension via a LPA-RhoA-ROCK signaling cascade. The stiffness of cells expressing $MRLC^{T18A}$ did not change on LPA stimulation. In contrast, the stiffness of cells expressing $MRLC^{WT}$ had increased. Immunofluorescence staining for PP-MRLC indicated that endogenous MRLC was diphosphorylated by LPA stimulation. The combination of urea- and SDS-PAGE showed that the there was no difference in the change of P-MRLC between the $MRLC^{T18A}$- and $MRLC^{WT}$-expressing cells by LPA stimulation. The endogenous MRLC in cells expressing dominant-negative RhoA was not diphosphorylated despite LPA stimulation. Treatment with both LPA and ML-7 revealed that ROCK diphosphorylated MRLC directly. These results suggest that the diphosphorylation of MRLC enhances the intracellular tension due to actomyosin contraction. A recent study showed that LPA treatment induced the phosphorylation of MRLC (both mono- and diphosphorylation of MRLC) in hepatic myofibroblasts, thereby increasing the contractile force and migration velocity (Tangkijvanich et al., 2003). In addition, ROCK is involved in the phosphorylation of MRLC and the regulation of cellular contractile force (Yee et al., 2001). The major difference between this study and ours lies in the revelation of the distinct role played by the diphosphorylation of MRLC.

There is a possibility that LPA stimulation increases the number of stress fibers; the

transition from the dephosphorylation to monophosphorylation of MRLC might induce the formation of new stress fibers. Our results indicate that in cells expressing $MRLC^{T18A}$, the contractile force at the cell center did not change despite the cell's capability of constructing additional stress fibers; moreover, in cells expressing $MRLC^{WT}$, the tension in the central area increased. Furthermore, a previous report showed that in cells stimulated by calyculin A—a serine/threonine phosphatase inhibitor—the amount of P-MRLC increased at the cell periphery but was unchanged at the center (Peterson et al., 2004). Taken together, it appears that stress fibers are not formed at the cell center by LPA stimulation; instead, these results strongly suggest that the transition from mono- to diphosphorylated MRLC enhances the tension acting on stress fibers.

Our results show that the diphosphorylation of MRLC by LPA stimulation was directly induced by the activation of ROCK, which agrees with previously reported results (Manning et al., 2000). ROCK can activate myosin II motor activity not only by inhibiting MRLC phosphatase (Kimura et al., 1996) but also by monophosphorylating (Amano et al., 1996) or diphosphorylating (Ueda et al., 2002) MRLC in a Ca^{2+}/calmodulin-independent manner. Although Ca^{2+}/calmodulin-dependent MLCK can diphosphorylate MRLC, the amount of calmodulin available for the phosphorylation of MRLC appears limited, even at high Ca^{2+} concentrations (Geguchadze et al., 2004). Therefore, we believe that the diphosphorylation of

MRLC mainly depends on Ca^{2+}/calmodulin-independent kinases such as ROCK, ZIP kinase (Murata-Hori et al., 2001), and citron kinase (Yamashiro et al., 2003). These kinases are localized at different sites in a cell. To control the contractile force in a cell spatiotemporally, the cells must utilize these kinases in different ways in order to phosphorylate MRLC depending on the physiological requirements. For example, citron kinase regulates cytokinesis (Madaule et al., 1998), and ZIP kinase is necessary for cell motility (Komatsu and Ikebe, 2004). These reports suggest that the diphosphorylation of MRLC is crucial in many physiological events, although the manner in which the functions of these kinases are coordinated in the cell is unclear. In future studies, we will focus on the spatiotemporal regulation of the phosphorylation of MRLC in eukaryotic cells.

ACKNOWLEDGMENTS

We are grateful to Dr. M. Matsuda (Osaka University) and thank him for his gifts. This work was supported by the Sasakawa Scientific Research Grant from the Japan Science Society and by a Grant-in-Aid from the Ministry of Education, Culture, Sports, Science and Technology of Japan (14GS0301 for K. K.).

LITERATURE CITED

Amano M, Ito M, Kimura K, Fukata Y, Chihara K, Nakano T, Matsuura Y, Kaibuchi K. 1996. Phosphorylation and activation of myosin by Rho-associated kinase (Rho-kinase). J Biol Chem 271(34):20246-20249.

Aoki K, Nakamura T, Matsuda M. 2004. Spatio-temporal regulation of Rac1 and Cdc42 activity during nerve growth factor-induced neurite outgrowth in PC12 cells. J Biol Chem 279(1):713-719.

Colburn JC, Michnoff CH, Hsu LC, Slaughter CA, Kamm KE, Stull JT. 1988. Sites phosphorylated in myosin light chain in contracting smooth muscle. J Biol Chem 263(35):19166-19173.

Daniel JL, Sellers JR. 1992. Purification and characterization of platelet myosin. Methods Enzymol 215:78-88.

Geguchadze R, Zhi G, Lau KS, Isotani E, Persechini A, Kamm KE, Stull JT. 2004. Quantitative measurements of Ca^{2+}/calmodulin binding and activation of myosin light chain kinase in cells. FEBS Lett 557(1-3):121-124.

Haga H, Sasaki S, Kawabata K, Ito E, Ushiki T, Sambongi T. 2000. Elasticity mapping of living fibroblasts by AFM and immunofluorescence observation of the cytoskeleton. Ultramicroscopy 82(1-4):253-258.

Ikebe M, Hartshorne DJ, Elzinga M. 1986. Identification, phosphorylation, and

dephosphorylation of a second site for myosin light chain kinase on the 20,000-dalton light chain of smooth muscle myosin. J Biol Chem 261(1):36-39.

Ikebe M, Koretz J, Hartshorne DJ. 1988. Effects of phosphorylation of light chain residues threonine 18 and serine 19 on the properties and conformation of smooth muscle myosin. J Biol Chem 263(13):6432-6437.

Kimura K, Ito M, Amano M, Chihara K, Fukata Y, Nakafuku M, Yamamori B, Feng J, Nakano T, Okawa K, Iwamatsu A, Kaibuchi K. 1996. Regulation of myosin phosphatase by Rho and Rho-associated kinase (Rho-kinase). Science 273(5272):245-248.

Komatsu S, Ikebe M. 2004. ZIP kinase is responsible for the phosphorylation of myosin II and necessary for cell motility in mammalian fibroblasts. J Cell Biol 165(2):243-254.

Krarup T, Jakobsen LD, Jensen BS, Hoffmann EK. 1998. Na^{+}-K^{+}-2Cl- cotransport in Ehrlich cells: regulation by protein phosphatases and kinases. Am J Physiol 275(1 Pt 1):C239-250.

Madaule P, Eda M, Watanabe N, Fujisawa K, Matsuoka T, Bito H, Ishizaki T, Narumiya S. 1998. Role of citron kinase as a target of the small GTPase Rho in cytokinesis. Nature 394(6692):491-494.

Manning TJ, Jr., Parker JC, Sontheimer H. 2000. Role of lysophosphatidic acid and rho in glioma cell motility. Cell Motil Cytoskeleton 45(3):185-199.

Matsumura F, Totsukawa G, Yamakita Y, Yamashiro S. 2001. Role of myosin light chain

phosphorylation in the regulation of cytokinesis. Cell Struct Funct 26(6):639-644.

Mizutani T, Haga H, Kawabata K. 2004a. Cellular stiffness response to external deformation: tensional homeostasis in a single fibroblast. Cell Motil Cytoskeleton 59(4):242-248.

Mizutani T, Haga H, Nemoto K, Kawabata K. 2004b. Wide-range scanning probe microscopy for visualizing biomaterials in the submillimeter range. Japanese Journal of Applied Physics Part 1-Regular Papers Short Notes & Review Papers 43(7B):4525-4528.

Murata-Hori M, Fukuta Y, Ueda K, Iwasaki T, Hosoya H. 2001. HeLa ZIP kinase induces diphosphorylation of myosin II regulatory light chain and reorganization of actin filaments in nonmuscle cells. Oncogene 20(57):8175-8183.

Nagayama M, Haga H, Kawabata K. 2001. Drastic change of local stiffness distribution correlating to cell migration in living fibroblasts. Cell Motil Cytoskeleton 50(4):173-179.

Nagayama M, Haga H, Takahashi M, Saitoh T, Kawabata K. 2004. Contribution of cellular contractility to spatial and temporal variations in cellular stiffness. Exp Cell Res 300(2):396-405.

Peterson LJ, Rajfur Z, Maddox AS, Freel CD, Chen Y, Edlund M, Otey C, Burridge K. 2004. Simultaneous stretching and contraction of stress fibers in vivo. Mol Biol Cell 15(7):3497-3508.

Radmacher M, Fritz M, Kacher CM, Cleveland JP, Hansma PK. 1996. Measuring the viscoelastic properties of human platelets with the atomic force microscope. Biophys J

70(1):556-567.

Somlyo AP, Somlyo AV. 2003. Ca^{2+} sensitivity of smooth muscle and nonmuscle myosin II: modulated by G proteins, kinases, and myosin phosphatase. Physiol Rev 83(4):1325-1358.

Tangkijvanich P, Melton AC, Santiskulvong C, Yee HF, Jr. 2003. Rho and p38 MAP kinase signaling pathways mediate LPA-stimulated hepatic myofibroblast migration. J Biomed Sci 10(3):352-358.

Trybus KM. 1989. Filamentous smooth muscle myosin is regulated by phosphorylation. J Cell Biol 109(6 Pt 1):2887-2894.

Ueda K, Murata-Hori M, Tatsuka M, Hosoya H. 2002. Rho-kinase contributes to diphosphorylation of myosin II regulatory light chain in nonmuscle cells. Oncogene 21(38):5852-5860.

Umemoto S, Bengur AR, Sellers JR. 1989. Effect of multiple phosphorylations of smooth muscle and cytoplasmic myosins on movement in an *in vitro* motility assay. J Biol Chem 264(3):1431-1436.

Yamashiro S, Totsukawa G, Yamakita Y, Sasaki Y, Madaule P, Ishizaki T, Narumiya S, Matsumura F. 2003. Citron kinase, a Rho-dependent kinase, induces di-phosphorylation of regulatory light chain of myosin II. Mol Biol Cell 14(5):1745-1756.

Yee HF, Jr., Melton AC, Tran BN. 2001. RhoA/rho-associated kinase mediates fibroblast

contractile force generation. Biochem Biophys Res Commun 280(5):1340-1345.

Yuasa HJ, Nakatomi A, Suzuki T, Yazawa M. 2002. Genomic structure of the sponge, Halichondria okadai calcyphosine gene. Gene 298(1):21-27.

FIGURE LEGENDS

FIGURE 1

Inhibition of MRLC diphosphorylation in cells overexpressing MRLC^{T18A}-GFP. **A:** Cells expressing MRLC^{T18A} were treated with or without 10 μM LPA and stained with anti-PP-MRLC after fixation. The bar denotes a length of 50 μm. **B:** The expression level of exogenous to endogenous MRLCs was analyzed by western blotting. Lysates from MRLC^{T18A}-GFP (T18A), MRLC^{WT}-GFP (WT), non-transfected (control) cells were subjected to SDS-PAGE. Proteins were monitored by anti-MRLC and anti-tubulin, respectively.

FIGURE 2

Change in the stiffness of cells expressing MRLC^{T18A}-GFP or MRLC^{WT}-GFP after LPA stimulation. **A:** Stiffness images were measured by an M-SPM before and after LPA stimulation. A significant increase in stiffness was observed in cells expressing MRLC^{WT} after LPA stimulation (arrows). On the other hand, MRLC^{T18A} expression suppressed the increase in stiffness after LPA stimulation. The bar denotes a length of 20 μm. **B:** The bar graph shows the averaged stiffness of the cells expressing MRLC^{T18A}-GFP or MRLC^{WT}-GFP before (–) and after (+) LPA stimulation. The details of the stiffness analysis have been described in the Materials

and Methods section. Data represent mean ± SE from six experiments (*$P < 0.01$).

FIGURE 3

Diphosphorylation of endogenous MRLC by LPA stimulation. **A:** The immunofluorescence micrographs show PP-MRLC (green) and filamentous actin (red) in LPA stimulated and unstimulated cells. The bar denotes a length of 50 μm. **B:** The intensity of PP-MRLC from the immunofluorescence micrographs (A) was averaged in each cell and is shown in the bar graph. Data represent mean ± SE from more than 30 cells (*$P < 0.001$).

FIGURE 4

Diphosphorylation and monophosphorylation of $MRLC^{T18A}$- or $MRLC^{WT}$-expressing cells by LPA stimulation. **A:** Cells transfected with $MRLC^{T18A}$ or $MRLC^{WT}$ were treated with LPA. The lysates from cells were subjected to urea-gel western blotting. Phosphorylated MRLCs were monitored by an antibody for P- and PP-MRLC (upper panel). The same amount of samples was subjected to SDS-PAGE and western blotting. The total MRLC was monitored by anti-MRLC (lower panel). **B:** The increase in P-MRLC in $MRLC^{T18A}$ or $MRLC^{WT}$ expressing cells was compared by statistical analysis (see materials and methods).

FIGURE 5

Functioning of ROCK as a kinase. The cells expressing Rho^{N19} were treated with 10 μM LPA and then stained with anti-PP-MRLC (A) after 30 min of LPA stimulation. The cells also express DsRed as an expression marker (B). Endogenous MRLC of cells expressing Rho^{N19} were not diphosphorylated by the LPA treatment. However, cells that did not express Rho^{N19} showed diphosphorylated MRLC (A). Cells stimulated with both LPA and ML-7 were stained with anti-PP-MRLC (C) and phalloidin (D). Each cell showed PP-MRLC in the stress fibers. Cells treated only with ML-7 were stained with anti-P-MRLC (E) and phalloidin (F). The bar denotes a length of 50 μm.

Fig. 1

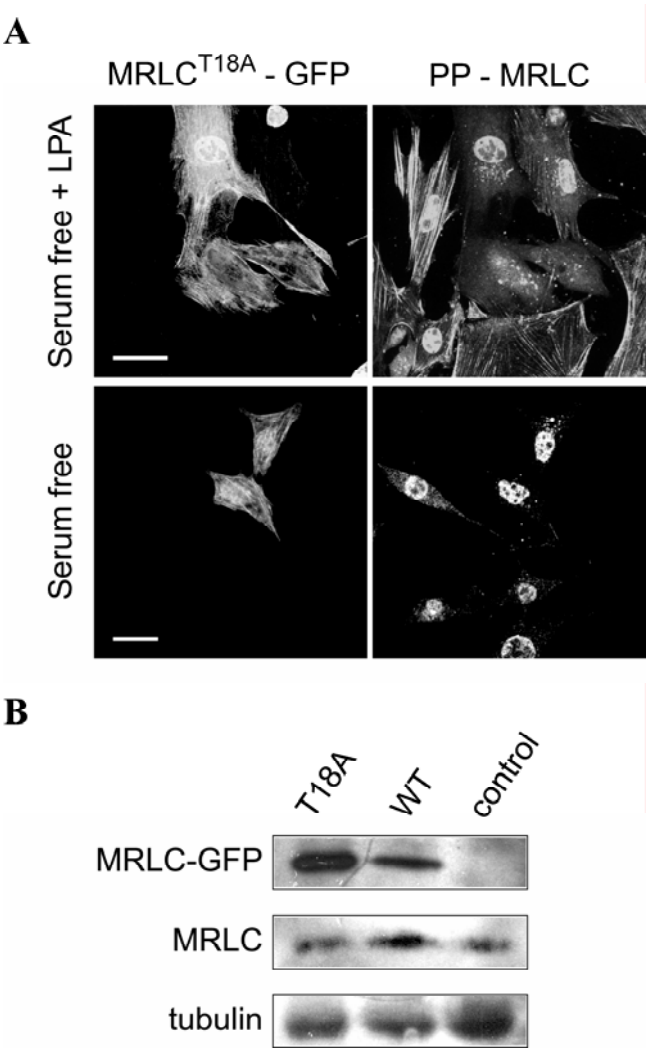
A
MRLC^{T18A} - GFP
PP - MRLC
Serum free + LPA
Serum free
B
T18A
WT
control
MRLC-GFP
MRLC
tubulin

Fig. 2

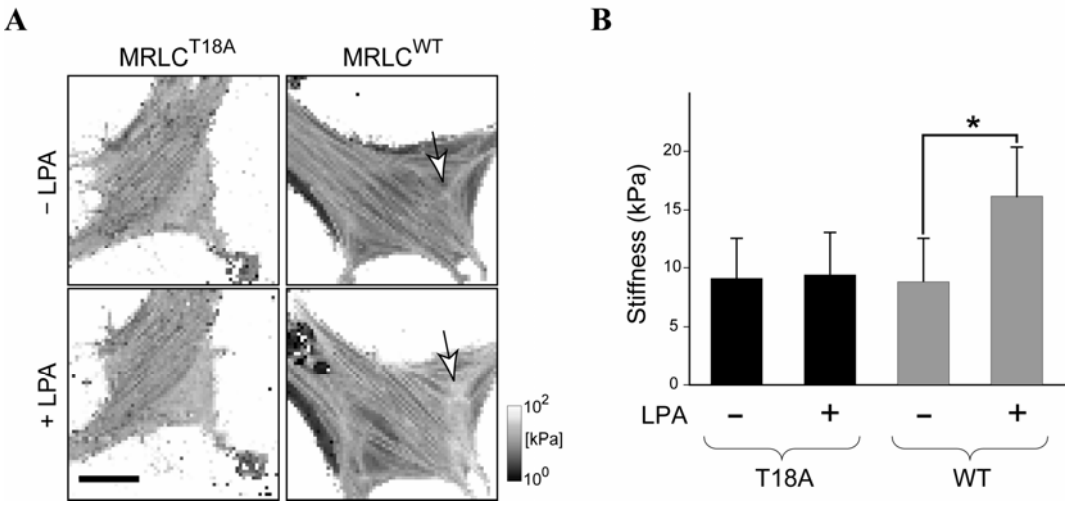
A
MRLC^T18A
MRLC^WT
– LPA
+ LPA
10^2
[kPa]
10^0
B
Stiffness (kPa)
20
15
10
5
0
*
LPA
–
+
–
+
T18A
WT

Fig. 3

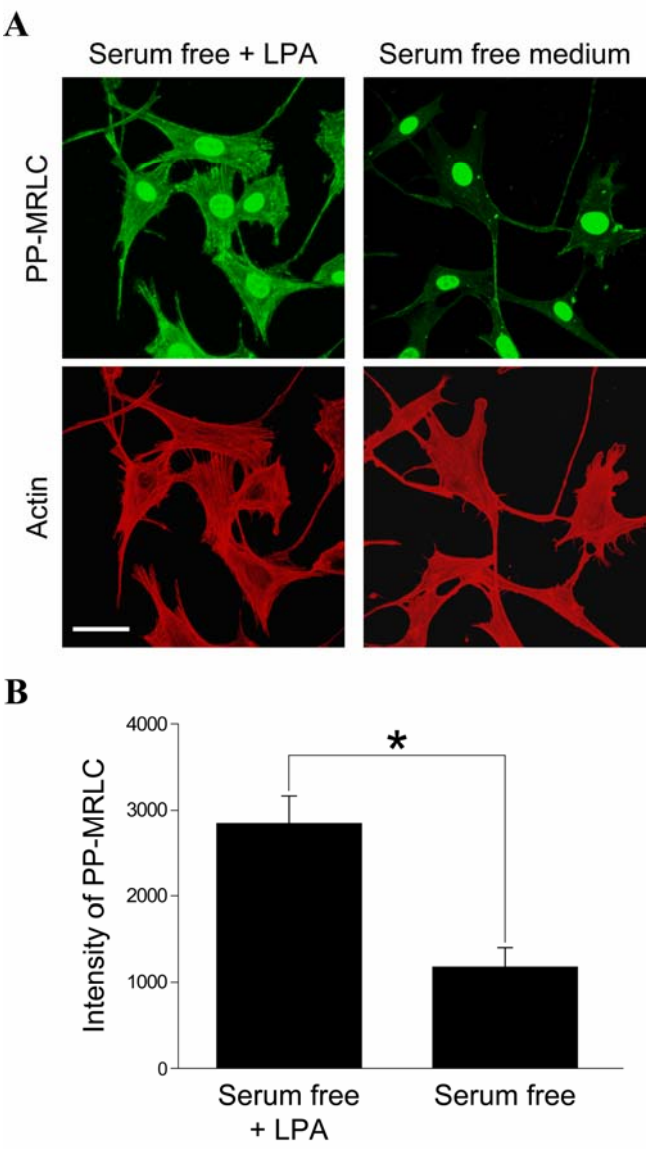
A
Serum free + LPA
Serum free medium
PP-MRLC
Actin
B
Intensity of PP-MRLC
4000
3000
2000
1000
0
*
Serum free + LPA
Serum free

Fig. 4

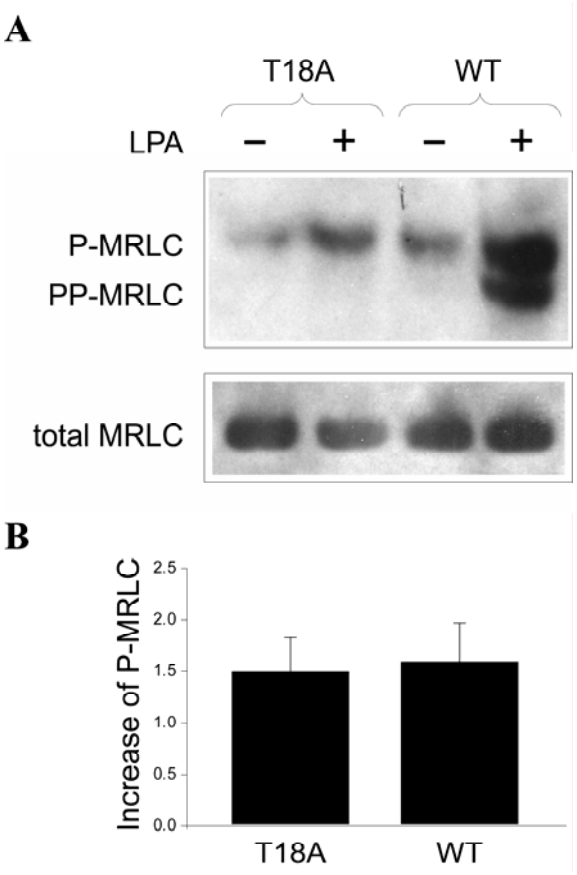
A
T18A
WT
LPA
–
+
–
+
P-MRLC
PP-MRLC
total MRLC
B
Increase of P-MRLC
2.5
2.0
1.5
1.0
0.5
0.0
T18A
WT

Fig. 5